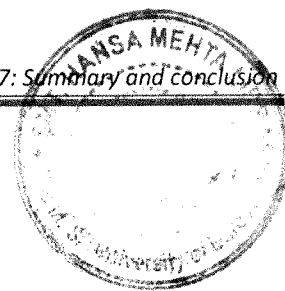




Summary & conclusions ●



7. SUMMARY AND CONCLUSION

7.1 Introduction

Cancer is a generic term for a large group of diseases that can affect any part of the body. Other terms used are malignant tumors and neoplasms. One defining feature of cancer is the rapid creation of abnormal cells that grow beyond their usual boundaries, and which can then invade adjoining parts of the body and spread to other organs. This process is referred to as metastasis. Metastases are the major cause of death from cancer. Cancer is a leading cause of death worldwide and accounted for 7.6 million deaths (around 13% of all deaths) in 2008.

Metastasis is the fatal stage in all cancer which remains incurable in spite of lots of research in recent scenario. Bone is the most prone site for metastasis because of its physiological environment which supports tumor inoculation and progress. Some commonly occurred human cancer such as prostate cancer, breast cancer, renal carcinoma, thyroid cancer and multiple myelomas have high vulnerability (more than 50% case) of metastasized at bone site at advanced stage. Because of complication of disease and incomplete understanding still hinder development of effective drug delivery to bone metastasis. The high rate of metastasis occurrence at bone is because of the reason that bone is a particularly 'fertile soil' for tumor cells to grow tumor by providing abundance growth factors secreted by osteoclast cell which promote tumor growth and metastasis progress.

BPs have strong affinity toward bone mass. All BPs distributed in bone very fast after injection and found in 100 times high concentration in bone in comparison to C_{max} concentration after injection and concentration remain high even after 6 month of injection. Because of its strong selectivity and affinity, BPs are now widely used as a bone imaging agents in conjugation with radiopharmaceuticals. Bisphosphonates, in addition to bone targeting ligand, work as a potent cytotoxic and antiangiogenic in nature which give added advantage of its usage.

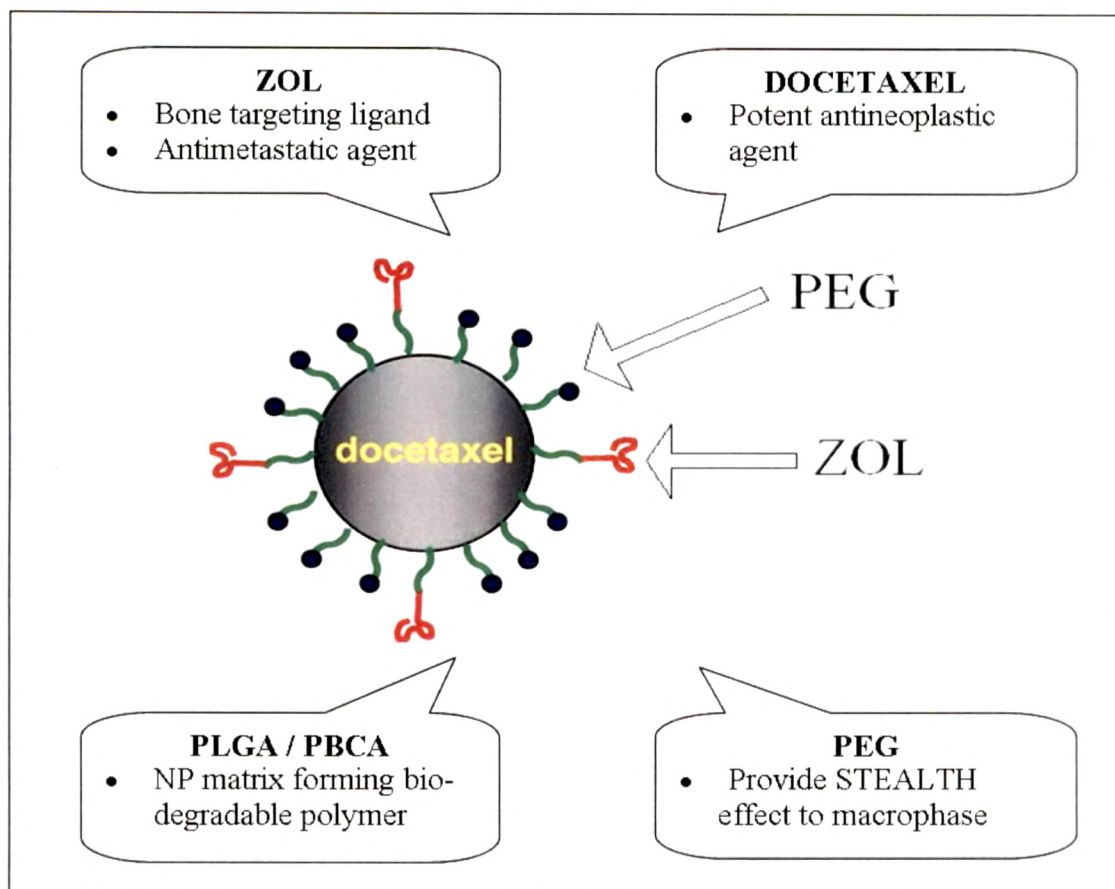


Figure 7.1: Strategy for bone metastasis targeted nanocarrier

So, it is hypothesized that the proposed nanoparticle based anticancer drug entrapped functionalized targeted system may target bone metastasis with synergistic effect on metastatic tumor by anticancer drug with bisphosphonate, reduce bone complication by controlling osteoclast activity by bisphosphonate, same time reduce further metastasis progress by reducing activation of growth factors by controlling osteoclast activity and reducing occult tumor cell count in blood.

7.2 Analytical methods

The docetaxel content was estimated using a HPLC method with UV-visible spectrophotometric detector. The separation was performed on a C 18 150-4.6 HPLC column with mobile phase consisted of acetonitrile: water mixture (70:30 v/v). The run

time was 15 min and the retention time of docetaxel was 4.47 min. UV detection wavelength was 230 nm and mobile phase flow rate 1 ml/min. Estimation of IPP and ApppI was performed using LC-MS method. The highly hydrophilic compounds were separated on a C18 reversed phase column using volatile dimethylhexylamine (DMHA) as an ion-pair agent. On-line HPLC-ESI MS measurements were carried out using an Agilent 6410 Triple Quad LC/MS for the analysis of IPP, ApppI and AppCCl2 (standard). Instrument was equipped with an electrospray ionization source (EIS) and operated on negative ion mode. For the Agilent triple quadrupole instrument optimized parameters were following: drying gas temperature was kept at 300°C, gas flow at 8 mL/min, nebulizer gas pressure operated at 40 psi and capillary voltage was kept at -4500V.

6-coumarine was estimated using fluorescence microplate reader (Perkin Elmer EnVision 2014 multilabel) equipped with a xenon lamp. The various experimental conditions like excitation wavelength and emission wavelength ($\lambda_{\text{emission}}$) were optimized ($\lambda_{\text{excitation}} = 430\text{nm}$; $\lambda_{\text{emission}} = 485$). Estimation of Poloxamer P188 was estimated using ammonium ferroisothiocyanate induced colorimetric measurement. The color intensity was measured at 510 nm in a spectrophotometer Shimadzu RF-540 spectrofluorometer. Method for PEG determination was carried out using NaOH degradation at higher temperature and prolong incubation followed by KI/I₂ induced colorimetric measurement by spectrophotometric at 500 nm. Content of zoledronic acid was determined using HPLC method with UV detector and C18 column. Mobile phase consisted of 2.5 L water, 4.7 mL formic acid and pH adjusted to 3.5 using sodium hydroxide with retention time of zoledronic acid was 1.00 min. UV detection wavelength was 210 nm and mobile phase flow rate 1 ml/min.

7.3 Formulation, development, characterization and stability studies

PLGA is a copolymer of lactic acid and glycolic acid. Depending on the ratio of lactide to glycolide, different forms of PLGA can be obtained, which are usually identified with regard to the monomers ratio used (e.g., PLGA 75:25 identifies as 75% lactic acid and 25% glycolic acid). PLGA is one of the most successfully used biodegradable polymers for the development of nanomedicines because it undergoes hydrolysis in the body to

produce the biodegradable metabolite monomers, lactic acid and glycolic acid, which are effectively processed by the body, resulting in minimal systemic toxicity (Wu, 1995).

PLGA-PEG conjugate was synthesized using N-Hydroxysuccinimide (NHS) and Dicyclohexylcarbodiimide (DCC) as an activator. Conjugation of ZOL with PLGA-PEG-NH₂ was performed using N,N'-Carbonyldiimidazole (CDI) as a conjugation linker. Conjugation was characterized using FTIR and NMR. DTX loaded PLGA NPs were prepared by solvent diffusion (nanoprecipitation) technique as described by Fessi et al., 1989.

The optimized batches of DTX loaded PLGA NPs (amount of PLGA 100mg, 0.5 % w/v poloxamer 188 and 2.5 as the ratio of aqueous to organic phase), PEGylated PLGA NPs and ZOL conjugated DTX loaded PEGylated PLGA NPs were characterized for particle size, entrapment efficiency and zeta potential. NPs demonstrated a mean hydrodynamic diameter below 150 nm with a polydispersity index of below 0.1 suggesting a uniform particle size distribution. Result demonstrates that with increase in PEG content particle size decrease with increase in entrapment due to micellar stabilization. PEG give amphiphilic nature and form micelle as a result particle size decrease with increase in % drug entrapment. Due to shielding of surface function group by PEG there is decrease in zeta potential. Conjugation reaction shows no change in the mean particle size of NPs. The EE (%) was found to be 73.53 ± 3.43 % in case of unconjugated NPs and PEGylated PLGA NPs exhibited a slight increase in entrapment efficiency where as ZOL conjugated NPs had an entrapment efficiency of 75.73 ± 4.38 % attributed to the loss of surface drug fractions during incubation and conjugation purpose. The zeta potential of ZOL conjugated nanoparticles (-26.33 ± 3.15) was slightly more negative than unconjugated (-4.38 ± 1.24) that can be attributed to charge contributed by ZOL. PEGylation of PLGA NP shows decrease in zeta potential due to charge shielding by PEG.

Aggregation resistance property of PEGylated and nonPEGylated PLGA NPs was determined using salt induced aggregation and serum induced aggregation methods. Results show that, among all formulations PLGA-PEG20 NPs and PLGA-PEG30 NPs displayed exceptionally high resistance to aggregation. The serum induced aggregation study showed that PLGA-PEG20 NPs and PLGA-PEG30 NPs did not show significant

increase in particle size, while the particle size of PLGA-PEG10 NPs and PLGA NPs increased dramatically with time.

In vitro bone affinity study was carried out to evaluate bone binding property of zoledronic acid before and after conjugation with PLGA NP. Zoledronic acid found to have strong bone binding affinity. Results demonstrated that more than 95% zoledronic acid was found with bone in bound form within 6 h. The affinity of zoledronic acid conjugated with PLGA NP also found only slight difference to free zoledronic acid. After 6 h zoledronic acid conjugated PLGA NP shown more than 90% bone binding affinity. The optimized batch of nanoparticles was lyophilized using different concentrations of sucrose, mannitol and trehalose. The redispersibility of the freeze-dried formulations and particle size of the nanoparticles before and after freeze-drying was measured and recorded. Hence trehalose was found to be the best as a cryoprotectant to preserve the initial properties of NPs suspension after freeze drying.

It can be observed that when stored at $5^{\circ}\text{C} \pm 3^{\circ}\text{C}$, NPs are stable up to a period of six months with no significant change in either particle size, zeta potential or the drug content. The short term studies also indicate that nanoparticle formulation when stored at $25 \pm 2^{\circ}\text{C}/60 \pm 5\% \text{RH}$ are also stable with no significant change in drug content. All the samples stored at $5^{\circ}\text{C} \pm 3^{\circ}\text{C}$ and $25 \pm 2^{\circ}\text{C}/60 \pm 5\% \text{RH}$ were redispersed easily within 2 minutes.

We can conclude that DTX can be effectively loaded into PLGA polymeric carriers and a particle size suitable for parenteral administration can be obtained. PEGylation and ZOL conjugation of PLGA NPs can be done effectively without significant change in morphology of the NPs. DTX entrapped PLGA NP formulation demonstrated a sustained release effect. PLGA based NP formulations found good stability while storage condition was refrigerated ($2 - 8^{\circ}\text{C}$).

The PBCA NPs are reported as a novel tool to deal with resistant cancer because of its unique drug delivery mechanism. Drug loaded in PBCA NP forms ions pairs with degraded polymer products at the physiological pH and thus protects the drug from getting effluxed out from intracellular domain by resistance mechanism of the P-

glycoprotein, i.e. MDR-1 type. Conjugation of ZOL with PEG bisamine was performed using N,N'-Carbonyldiimidazole (CDI) as a conjugation linker in distilled DMF with triethylamine (TEA).

PBCA NPs were prepared by modified anionic polymerization technique described by Mitra and Lin with some modifications (Mitra and Lin, 2003). Briefly, NPs were prepared in an acidic polymerization medium (pH 1.5-3) containing poloxamer 188 as a stabilizer. The NP formation is by micellar emulsification process. PBCA-PEG NPs were prepared in similar manner as in case of PBCA NP with addition of mPEGamine and PBCA-PEG-ZOL NP was prepared using ZOL-PEG-amine as initiator in acidic polymerization medium respectively. Amine group of PEG work as nucleophilic initiator of polymerization reaction and propagated by micellar emulsification process while later turn to nanoparticle formation.

Prepared method also gives good entrapment with DTX because of emulsion micelles formation. Characterization of NP as PEGylation result also found satisfactory and found suitable for parenteral administration. PEGylation and ZOL conjugation of PBCA NPs can be done effectively without significant change in morphology of the NPs other than particle size and zeta potential. The ratio of PEGylation can be control by adjusting feed ratio of PEG to monomer. Ratio of monomer to PEG is very crucial in case of bisamine-PEG for type of block formed. At low PEG mol. concentration (< 50% to monomer conc.), it forms tri-block while at high (> 50% to monomer conc) it preferably forms diblock copolymer. With triblock formation the zeta potential reduce which gives strong speculation about flower configuration of triblock where PEG graft give nonflexible tight shielding on surface which effectively hides negativity and surface largely exposed with bended PEG chain which is electro-neutral in nature. The NP formation is directed by micelles formation which is self stabilized system without any need of surfactant.

Drug release from biodegradable polymeric nanoparticles depends on the Fickian diffusion through the polymer matrix and on the degradation rate of the polymer. In addition presence of larger quantity of hydrophobic drugs like DTX would contribute to increased hydrophobicity of the polymer matrix resulting in the increased barrier for water and hydroxyl ions to cause degradation of PBCA polymer (Huanga et al, 2007).

Therefore, the relative drug release rate decreases with increasing DTX content in particles has been observed. Results of Salt aggregation study showed that out of all formulation PBCA-PEG20 NPs and PBCA-PEG-PBCA NPs displayed exceptionally high resistance to aggregation. Results of serum induced aggregation showed no significant increase in particle size with PBCA-PEG20 NPs and PBCA-PEG-PBCA NPs, PBCA-PEG10 NPs showed slight increase with time while PBCA-PEG5 NPs and PBCA NPs showed dramatic increase in particle size with time. Zoledronic acid found to have strong bone binding affinity. Result of bone binding affinity study demonstrated that more than 95% zoledronic acid was found with bone in bound form within 6 h. After 6 h zoledronic acid conjugated PBCA NP shown more than 90% bone binding affinity.

Aggregation and drug leaching is a common problem in case of nanoparticulate dispersions as observed from the results. Hence, the dispersions are lyophilized in presence of cryoprotectants to maintain the stability of the dispersions on freeze drying. Trehalose was found to be the most effective cryo-protectant for lyophilization of the PBCA NPs at a NP: Sugar ratio of 1:5. Stability study of PBCA NP shows that when stored at $5^{\circ}\text{C} \pm 3^{\circ}\text{C}$, NPs are stable up to a period of six months with no significant change in either particle size, zeta potential or the drug content. The short term studies also indicate that nanoparticle formulation when stored at $25 \pm 2^{\circ}\text{C}/60 \pm 5\% \text{RH}$ are also stable with no significant change in drug content. All the samples stored at $5^{\circ}\text{C} \pm 3^{\circ}\text{C}$ and $25 \pm 2^{\circ}\text{C}/60 \pm 5\% \text{RH}$ were redispersed easily within 2 minutes.

7.4 In vitro cell line studies

After the preliminary studies at formulation preparation and characterization, the final objective was to deliver these nanoparticulate carriers by parenteral route to animals. But before the animal studies, the formulations should be evaluated for their safety and efficacy at tissue culture level. The aim of the study was to evaluate prepared NPs for cancer chemotherapy with a view to explore the possible effects of particle size, conjugation and particle surface coating on the cell uptake. Hence, the cell uptake, phagocytosis, cell cycle analysis, apoptosis and cytotoxicity studies were taken up prior to in-vivo studies. Cell uptake studies were carried out using 6-coumarin (lipophilic

fluorescent dye) loaded NPs with the aim of finding whether the NPs are internalized into the cells and to determine the intracellular concentrations of the loaded dye. The inhibition of FPP synthase by ZOL causes accumulation of isopentenyl pyrophosphate (IPP), which further converted to ApppI were estimated using LC-ESI-MS in MCF and BO2 cell lines.

For further in vitro antiopsonization evaluation, cell up take study was performed with mouse macrophage cell line RAW264. Results shows that in all formulations, PLGA-PEG30 NP and PLGA-PEG20 NP showed least phagocytic uptake in all time points which is five times less in compare to PLGA NP. Although, PLGA-PEG30 NP shows no added advantage of increase in PEG grafting over PLGA-PEG20 NP. Results showed, among the tested PBCA formulations, PBCA-PEG20 showed least phagocytic uptake and the decrease is about seven times less in comparison to PBCA NP. PBCA-PEG10 and PEG-PBCA-PEG also displayed moderate resistance to phagocytosis as the cellular uptake is about three times less than PBCA NP.

In MCF7 cell line, uptake of PLGA-PEG-ZOL NPs was found 32.77% that is higher as compared to PLGA-PEG20 NP at 30 min time point. The increased uptake at 60 min and 120 min time points was found to be 34.08% and 37.4%, respectively. In case of BO2 cell line internalization of PLGA-PEG-ZOL NPs was enhanced up to 36.51% in comparison to PLGA-PEG20 NP at 30 min time point. After 60 min and 120 min the increase in uptake is 27.16% and 30.32% in comparison to PLGA-PEG20 NP. In case of MCF-7 cell line, uptake of PBCA-PEG-ZOL NPs after 30 min was found to be 82.54% which is 1.62 times higher than PBCA-PEG NPs. In BO2 cell line, across all time points, the uptake of PBCA-PEG-ZOL NPs was found to be more than 1.4 times higher than PBCA-PEG NPs.

PLGA-PEG-ZOL NP uptake can be block by using both inhibitor simultaneously but not by individual, thus it display that PLGA-PEG-ZOL NP uptake routed by both clathrin mediated and caveolae mediated endocytosis where one pathway compensate NP uptake when second pathway got blocked. Result demonstrated that PBCA-PEG-ZOL NP uptake was reduce but can't block completely by using both inhibitor simultaneously or by individual, thus it display that PBCA-PEG-ZOL NP uptake routed by both clathrin

mediated and caveolae mediated endocytosis, but there is chance of involvement of other pathway as well.

Confocal study confirmed high degree of relevance with route characterization results where PLGA-PEG-ZOL NP found with very few colocalization demonstrated that NPs got endocytosis by both clathrin mediated and caveolae mediated endocytosis mechanism where caveolae pathway follow non-lysosomal route. PLGA-PEG20 NP follows predominantly to lysosome through early endosomes which displayed significant colocalization of NPs with lysosomes. Confocal study with PBCA NPs demonstrates that PBCA-PEG-ZOL NPs were endocytosed by both clathrin mediated and caveolae mediated endocytosis mechanism, where caveolae pathway followed a non-lysosomal route. PBCA-PEG20 NPs followed to lysosome through early endosomes which displayed few co-localization of NPs and lysosomes.

Intracellular retention study demonstrated that after 60 min, % retention of PLGA-PEG-ZOL NP in BO2 cell line was found 24.38% more in comparison to PLGA-PEG20 NP. PBCA-PEG-ZOL NP in BO2 cell line demonstrated that after 60 min, % retention was found 49.15% in comparison to PBCA-PEG20 NP having 24.14% NP remaining intracellularly. The IC₅₀ value for BO2 cells treated with PLGA-PEG-ZOL NPs was found to be 1.06 nM after 48 h that was 5.45 and 2.84 times less than DTX, DTX loaded PLGA-PEG NPs respectively. Exposure for 72 h further lowered the IC₅₀ value by 1/3rd of its value to 0.32, which was more than 10 times less in comparison with DTX solution. The IC₅₀ value for MCF-7 cells treated with PBCA-PEG-ZOL NPs was found to be 2.49 nM after 48 h that was 2.6, 2.7 and 1.4 times less than DTX, DTX-ZOL and PBCA-PEG NPs respectively. Exposure for 72 h further lowered the IC₅₀ value by 1/5th of its value to 0.46, which was more than 11 times less in comparison with DTX solution. The IC₅₀ value for BO2 cells treated with PBCA-PEG-ZOL NPs was found to be 0.36 nM after 72 h which was 9.4, 9.0 and 7.2 times less than DTX, DTX-ZOL and PBCA-PEG NPs.

Cell cycle analysis has been performed by FACS using PI staining in BO2 cell line after treatment with DTX, DTX loaded PLGA-PEG20 NP and PLGA-PEG-ZOL NPs. The PLGA-PEG-ZOL NPs showed significant increase in amount of apoptotic cells at Sub

G0/G1 phase (2 times and 4 times as compared to PLGA-PEG NPs and DTX, respectively). After treatment with PBCA-PEG-ZOL NPs, blockage at G2/M check point does not change significantly as DTX and PBCA-PEG NPs treatment with significant change in amount of apoptotic cells at Sub G0/G1 phase showing more and more cells underwent apoptotic cell death (2.5 times and 6.2 times as compared to PBCA-PEG NPs and DTX, respectively) which signifies effectiveness of PBCA-PEG-ZOL NPs as an effective carrier for DTX among tested formulations.

Apoptosis study of prepared NPs was conducted using Annexin V staining procedure in MCF7 and BO2 cell lines. In MCF7 cell line, DTX loaded PLGA-PEG-ZOL NPs were able to cause a significant increase in programmed cell death as 32.58% cells were observed in late apoptotic phase in comparison to 14.72% and 23.03% cell death when treated with DTX and DTX loaded PLGA-PEG NPs. In case of BO2 cell line, DTX loaded PLGA-PEG-ZOL NPs showed 34.39% cells at late apoptosis as compared to DTX solution (7.46%) and DTX loaded PLGA-PEG NPs (22.64%). In MCF-7 cells, DTX loaded PLGA-PEG NPs showed almost 2 times pro-apoptotic cells (3.97%) whereas DTX loaded PLGA-PEG-ZOL NPs showed 7.79% cells within pro-apoptotic phase. IN BO2 cell line, DTX loaded PBCA-PEG-ZOL NPs showed 36.39% cells with late apoptosis as compared to DTX solution and DTX loaded PBCA-PEG NPs which found only 7.46% and 20.9%, late apoptotic cell death respectively.

The molecular mechanism of action of the N-BPs (such as zoledronic acid, ZOL) is *via* inhibition of the FPP synthase, the key enzyme of the mevalonate pathway, in particular, due to consequent depletion of prenylated GTPases. However, accumulation of the unprenylated GTPases and subsequent inappropriate activation of downstream signaling pathways may also account for the anti-resorptive effect of N-BPs rather than loss of the prenylated proteins. The inhibition of FPP synthase by N-BPs, in addition to depletion of the biosynthesis of FPP and GGPP, leads to accumulation of the early metabolites of mevalonate pathway, IPP and ApppI which found cytotoxic in nature. On-line HPLC-ESI MS measurements were carried out using an Agilent 6410 Triple Quad LC/MS for the analysis of IPP, ApppI and AppCCI2 (standard). Instrument was equipped with an electrospray ionization source (EIS) and operated on negative ion mode.

Results showed that treatment with ZOL solution in MCF-7 cell line found to increase IPP production more than 19 times than control group treated with PBS. Treatment with PBCA-PEG-ZOL NPs showed 7 times increase in IPP production in comparison to ZOL solution treatment and 138 times higher than control group. ApppI level in MCF-7 cell line after treatment with PBCA-PEG-ZOL NPs was found 5.3 times higher than treatment with ZOL solution. In case of BO2 cell line, IPP production after treatment with PBCA-PEG-ZOL NPs was 5.35 times higher than ZOL solution and IPP level in control group was below detection level. However, no ApppI production in BO2 cell line after treatment with PBCA-PEG-ZOL NPs and ZOL solution was found.

7.5 In vivo pharmacokinetic and biodistribution studies

Labeling of the PLGA and PBCA NP with radioisotopes was carried out by tagging with suitable gamma emitting radioisotope such as ^{99m}Tc . The prepared ^{99m}Tc -NPs complex was tested for labeling efficiency using TLC method. All formulations, DTX (98.2%), PLGA NP (99.1%), PLGA-PEG20 NP (98.7%) and PLGA-PEG-ZOL NP (99.4%) found high labeling efficacy as more than 98% activity found at base (lower $2/3^{\text{rd}}$). Radiolabeled complex of ^{99m}Tc -formulations of 100 μL of radiolabeled complex of ^{99m}Tc -solution was injected through tail vein of the mice. Blood was withdrawn by cardiac puncture after different time interval and the mice were sacrificed by cervical dislocation. Major organs (blood, heart, liver, spleen, kidney, lungs, tumor, intestine, stomach, tumor, tumor bearing bone, bone without tumor, tail, and brain) were isolated weighed and radioactivity present in each tissue/organ was measured using shielded well-type gamma scintillation counter. Radiopharmaceutical uptake per gram in each tissue/organ was calculated.

From the results of blood to liver NP distribution ratio, significant change could be observed in distribution of all NP formulations in blood and liver compartment which further increases with time. At 1 h time point, distribution ratio of PLGA-PEG20 NP is 2.15 fold higher than distribution ratio of PLGA NP (Table 6.6(a), fig. 6.1(a)). At 4 h time point, the distribution ratio was increased to 3.22 fold and even at 24 h time point it was increased considerably to 5.05 fold. Results clearly demonstrated that PLGA-PEG20 NP remains in blood for prolonged time in comparison to PLGA NP that retained more in

liver. In case of ^{99m}Tc labeled PLGA NP and PBCA NP, liver and spleen accumulated a major portion of the administered radioactivity as they are the two major organs of reticulo-endothelial system (RES) which are known to accumulate and metabolize foreign particle.

Bone targeting affinity of PLGA-PEG-ZOL NP was determined from the ratio of NP distribution at tumor bearing bone in comparison to concentration in blood. The ratio of NP concentration in bone to blood was 50 fold higher with PLGA-PEG-ZOL NP than with PLGA-PEG NP after 24 h. At 1 h and 4 h time point, the distribution ratio was approximately 8 fold (780.6%) and 33 fold (3279%) accordingly. PLGA-PEG-ZOL NP distribution in tumor infected bone is also significantly high in comparison to normal bone. After 24 h the change in distribution was 3.5 fold higher (342.8%) in tumor bone than normal bone (table 6.6). The NP distribution at 1 h was 2.5 fold higher (250%) and at 4 h time point it was found to be 2.9 fold higher (290.0%) which show better deposition of PLGA-PEG-ZOL NP at infected bone than normal bone. The tumor retention in comparison to blood for PLGA-PEG-ZOL NP was significantly higher (504%) than for PLGA-PEG20 NP after 24 h. At 1 h (312.2%) and 4 h (358.6 %) the retentions were also relatively high.

Stability of prepared ^{99m}Tc -PBCA NPs complex was tested for labeling efficiency using ITLC method. PBCA NP (98.57%), PBCA-PEG20 NP (98.19%) and PBCA-PEG-ZOL NP (98.21) found high labeling efficacy as more than 98% activity found at base (lower 2/3rd). From the results of blood to liver NP distribution ratio, significant change can be observed in distribution of both NPs formulation in blood and liver compartment which further increasing with time. At 1 h time point, distribution ratio of PBCA-PEG20 NP is 3 fold high than distribution ratio of PBCA NP. At 4 h time point, the distribution ratio change to four fold and even at 24 h time point it change considerably to more than 6 fold. Results clearly show that PBCA-PEG20 NP remains in blood for prolong time in comparison to PBCA NP.

Biodistribution of various PBCA NP formulations was evaluated for bone targeting affinity. For comparison of radio-distribution, results were also presented as ratio of

distribution between two organs. The ratio of NP concentration in bone to blood was 39 fold higher for PBCA-PEG-ZOL NP than PBCA-PEG20 NP after 24 h. At 1 h and 4 h time point, the distribution ratio was approximately 8 times (794.12%) and 25 fold higher (2506.33%) accordingly. PLGA-PEG-ZOL NP distribution in tumor infected bone is also significantly high in comparison to normal bone. After 24 h the change in distribution was 3 fold (301.39%) higher in tumor bone than normal bone. The NP distribution at 1 h (250.0%) and at 4 h (300.0%) was also show better deposition of PLGA-PEG-ZOL NP at infected bone than normal bone. The tumor retention in comparison to blood for PBCA-PEG-ZOL NP is significantly high (254%) than for PBCA-PEG20 NP after 24 h. At 1 h (185%) and 4 h (251%) the retention are also relatively high. The results showed that ZOL had more affinity toward infected bone than normal bone because of ZOL enhanced NP retention at tumor site. Same time, PBCA-PEG-ZOL NP shown good bone and tumor uptake in comparison to PBCA-PEG20 NP.

7.6 Conclusion

ZOL anchored, PEGylated and DTX entrapped PBCA and PLGA NP have display potential characteristic as delivery system. *In vitro* phagocytic studies also confirmed effectiveness of PEG coating in repelling phagocytic process. Various *in vitro* cell line study demonstrated effectiveness of this carrier as a nanocarrier for drug delivery. *In vitro* cell line studies such as cytotoxicity, apoptosis and cell cycle analysis shows enhanced activity with ZOL anchored NPs in comparison to other formulations tested. NPs uptake, uptake route characterization, NPs retention and confocal microscopy revealed change in uptake route of NPs in presence of ZOL. BO2 cell line, having morphology similar to bone metastasis found more prone to ZOL anchored NPs than MCF-7 cell line. ZOL was found to block mevalonate pathway which was a characteristic mechanism of bisphosphonate group. ZOL anchored PLGA NPs and PBCA NPs showed significant increase in retention of apoptotic byproducts such as ApppI and IPP than ZOL alone.

The outcomes showed that ZOL had more affinity toward infected bone than normal bone that enhanced NP retention at tumor site. Bone always cover with bone lining cells which prevent ZOL binding to bone to some extent, but when the active remodeling start in some disease such as osteoporosis, bone metastasis or bone tumor, the bone lining

layer largely removed for active bone remodeling. ZOL have more affinity toward open bone remodeling site and get accumulated and stay for prolong time.

Pharmacokinetic study for ZOL was carried out by Tianling Chen et al and reported that the 40% of ZOL was excreted after 24 h and 50% after 6 months. In report it was found that concentration of ZOL in bone was found more than 100 times of plasma C_{max} all the time point tested. Similar trend was also found in our study that the ZOL tagged NPs were found in very high concentration in bone than other organs, tissue or blood. The remarkable targeting efficiency resulted because of affinity of ZOL anchored NP toward infected bone site that make more NPs available for tumor retention and get internalized by endocytosis that enhanced in the presence of ZOL.

In vivo animal study using ^{99m}Tc radiolabeling was shown prolonged blood circulation half life, less liver uptake, higher retention of ZOL tagged NPs at bone site with enhanced tumor retention. The remarkable targeting efficiency was resulted because of affinity of ZOL anchored NP toward bone and tumor site. In this research we found enhanced targeting ability of PLGA-PEG-ZOL NPs and PBCA-PEG-ZOL NPs due to their strong affinity toward infected bone, EPR effect, prolong circulation half life as well as enhanced endocytosis. Thus, here we conclude that ZOL anchored PLGA NPs work as a novel tool for bone targeting and can be used to deliver therapeutics successfully in conditions such as bone tumor, bone metastasis or other bone diseases.